Colloids and Surfaces A: Physicochem. Eng. Aspects 477 (2015) 26–34

Contents lists available at ScienceDirect

Colloids and Surfaces A: Physicochemical and Engineering Aspects

journal homepage: www.elsevier.com/locate/colsurfa

Application of guanidine-containing polymers for preparation of pH responsive silica-based particles for drug delivery systems

Alexander S. Timin[a,*], Elena V. Balantseva[b], S. Yu. Khashirova[c], E.V. Rumyantsev[a], Tatiana Yu. Osadchaya[a]

[a] Inorganic Chemistry Department, Ivanovo State University of Chemistry and Technology (ISUCT)„ 7, Sheremetevsky Prosp., 153000, Ivanovo, Russian Federation
[b] Università di Torino, Dipartimento di Chimica and NIS (Nanostructed Interfaces and Surfaces) Centre, Via P. Giuria 7, 10125 Torino, Italy
[c] Kabardino Balkar State University, ul. Chernyshevskogo 173, Nal'chik, 360004 Kabardino Balkaria, Russian Federation

HIGHLIGHTS

- Hybrid materials based on silica particles and guanidine containing polymers were synthesized via sol–gel method.
- Polymer grafting influences pH-response and surface properties of final products substantially.
- Anionic (sulfasalazine) and cationic (doxorubicin) drugs were effectively loaded into polymer coated silicas.
- The drug loading and drug release were pH dependent and affected by the nature of grafted polymer and its content.

GRAPHICAL ABSTRACT

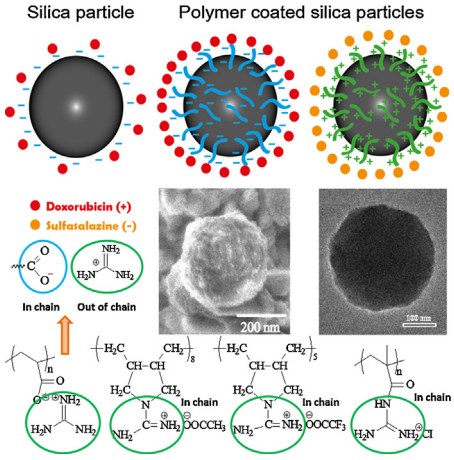

ARTICLE INFO

Article history:
Received 16 December 2014
Received in revised form 18 March 2015
Accepted 20 March 2015
Available online 2 April 2015

Keywords:
Polymer coating
Sol–gel
Drug delivery
Silica nanoparticles
Doxorubicin
Sulfasalazine

ABSTRACT

Guanidine containing polymers were applied to prepare polymer coated silica particles via a sol–gel method as potential candidates for drug encapsulation. Here, we used four types of grafted polymers for surface modification. The grafting amount was evaluated by thermogravimetric and elemental analysis and was in 18–34% range. Also polymer coated silica particles were characterized by Fourier transform infrared spectroscopy, differential scanning calorimetry and high resolution electron microscopy. The effect of grafted polymers on particle properties and pH-response has been reported. Anionic (sulfasalazine) and cationic (doxorubicin) drugs were effectively loaded into polymer coated silicas. The drug loading and drug release were pH dependent and affected by the nature of grafted polymer and its content. The properties revealed for investigated system have shown promising results for drug delivery with pH controllable drug release.

1. Introduction

Over the last decades, interest in a controlled drug delivery system (CDDS) is rapidly increased because of its application in

* Corresponding author. Tel.: +7 910 669 36 43.
E-mail address: a_timin@mail.ru (A.S. Timin).

http://dx.doi.org/10.1016/j.colsurfa.2015.03.037
0927-7757/

chemotherapy. This method is widely used to prevent cancer cells from dividing, multiplying and spreading throughout the body [1,2]. Many researchers concentrate on design of new materials and their application in drug-delivery systems [3–7]. Up to date, a lot of organic and inorganic materials have been synthesized and used as drug carries in CDDS [8,9]. One of the widely used materials is silica nanoparticles due to their unique features such as high surface area, thermal and chemical stabilities. Given the background, there are several strategies that can be used to improve drug loading efficiency. The first strategy is to design mesoporous silica nanoparticles with controlled pore sizes [10]. It was shown that the drug release is pore-size-dependent [11]. Gao has obtained hollow mesoporous silica nanoparticles with three pore sizes to control drug release rate and found out that drug-loaded mesoporous silica demonstrated not only pH-responsive release character but also exhibited pore-size-dependence. It has already been reported about preparation of mesoporous silica nanoparticles with definite pore size and their application in drug encapsulation and drug release [12–14].

Another strategy is based on surface functionalization of silica nanoparticles as a multifunctional platform for different drugs [14]. In this approach, organosilanes with different functional groups were successfully applied for surface functionalization. For instance, silica particles modified with phosphorous groups were prepared using 3-trihydroxysilylpropyl methylphosphate [15]. Such material contains negatively charged phosphate groups providing good ability to adsorb cationic drugs such as doxorubicin. The positive effect of grafted carboxylic [16], amino [17], trimethylammonium [18] groups on drug loading efficiency was also demonstrated. However, for the past two decades, polymers are being extensively used for surface modification and in drug delivery systems as well [19,20]. The main principle of application of such polymers is as follow: in aqueous media, the ionic polymer dissociates to form polyanion or polycation; the functional groups of such polymer ionize which leads to developing of fixed charge on the polymer network. The charge distribution depends on pH value in solution that is key aspect for pH-controlled drug release. Many polymers have been synthesized and applied for silica functionalization. The most common studies of ionic polymers include poly(acrylamide) [21], polyethilenglycol [22], polyacrilic acid [23]. However, there are only few studies concerning investigation and application of guanidine-containing polymers excepting polyhexamethylenguanidine and its analogues [24]. Taking into account the published results, we suggest that such polymers are one of the most promising candidates for silica modification thank to their low hemotoxicity and high ionic properties [25,26]. Moreover, it was shown that guanidine polymers performed better in comparison to their amine equivalents due to capability of binding guanidine groups stronger with negative molecules compared to amine groups [25,27]. An important aspect is their behavior in drug-delivery systems. For this reason, we chose several guanidine containing polymers based on polyacrylate, polydiallyl and polymethacryloyl guanidine. These polymers were synthesized via free radical polymerization. However, the polymerization rate of diallyl guanidine is quite slow and as a result we are able to obtain only polymer with low molecular weight [24]. In case of other polymers a degree of polymerization can be controlled and it is possible to synthesize polymers with different molecular weight. From the analysis of NMR and IR-spectra, typical resonance structures of guanidine-containing monomers and polymers are presented in Fig. 1. The third characteristic structure is most predominant for polyacrylate guanidine.

The aim of this work was to prepare polymer coated silica particles by co-condensation of tetraethooxysilane (TEOS) modified with guanidine-containing polymer using sol–gel method and to test them for drug encapsulation. Doxorubicin (positively charged drug) and sulfasalazine (negatively charged drug) were chosen as model drugs to assess the drug loading and releasing behavior of polymer coated silica particles. Herein, we reported application of guanidine-containing polymers grafted onto silica for development of pH-responsive hybrid materials for effective loading and control release of drugs. The full characterization of these materials including morphological, thermal and surface charge features were presented and discussed in details.

2. Experimental

2.1. Chemicals

TEOS ($Si(OC_2H_5)_4$, 98%) and ammonia solution (25 wt.%) were purchased from commercial chemical Company "Ecos-1" (Russian Federation). Doxorubicin (>98%) and sulfasalazine (98%) were purchased from Sigma–Aldrich. The guanidine containing polymers: PDAGA (M_w = 1594.02 g/mol), PDAGTFA (M_w = 1266.12 g/mol), PMCGH (M_w = 15051.66 g/mol), and PAG (M_w = 12064.24 g/mol) were provided by the department of macromolecular compounds of the Kabardino-Balkar State University and by the department of Chemistry of polyelectrolytes and biomedical polymers of A.V. Topchiev Institute of Petrochemical Synthesis, Russian Academy of Science. All chemicals were analytical grade and used without further treatment.

2.2. Preparation of polymer coated silica nanoparticles

The silica nanoparticles (SiNP) were prepared according to the sol–gel method described in [28]. Briefly, 8.57 mL of TEOS was mixed with 20 mL of water–ethanol (14%) solution and stirred for 5 h. The ammonia solution (pH 9) was added as a base catalyst. Polymer coated silica particles were synthesized by Stöber method: 10 mL of water solution containing definite concentration of polymer ($C_{polymer}$, Table 1) was mixed with 8.57 mL of TEOS to obtain a reaction mixture, which was stirred for 5 h under basic condition (pH 9). Then, this mixture was transferred into a Petri dish and was aged until the formation of the solid products. The solid phase was separated by centrifugation and washed with distilled water to remove unreacted reagents. After that, it was dried under vacuum at 105 °C for 3 days. The silica particles with the lowest and highest amount of grafted polymer were labeled "1" and "3", respectively. The amounts of TEOS, H_2O and polymers which were used for sol–gel synthesis with actual and percent yields are given in Table 1.

2.3. Doxorubicin loading

Typically, 1 mL of 0.5 mg/mL of doxorubicin was mixed with 3 mL of phosphate buffer solution (PBS, pH 7.4) containing 10 mg of dispersed polymer coated SiNPs. The mixture was shaken during 20 h at room temperature and then centrifuged during 10 min at 132,000 rpm to remove the solid phase. The amount of doxorubicin adsorbed was analyzed by measuring of its absorption in supernatant solution at the wavelength of 485 nm, which next allows to calculate the unloaded quantity of doxorubicin. In study of the pH influence on the doxorubicin loading, distilled water instead of PBS was used. The suitable value of pH was adjusted by NaOH or HCl solution.

2.4. Sulfasalazine loading

Firstly, a saturated sulfasalazine aqueous solution was prepared as described in [18]. Briefly, 0.5 g of sulfasalazine was dissolved in 1 L of water under stirring for 6 h. The residual solids were filtered. In this way prepared solution contains 75 μM of sulfasalazine. Due

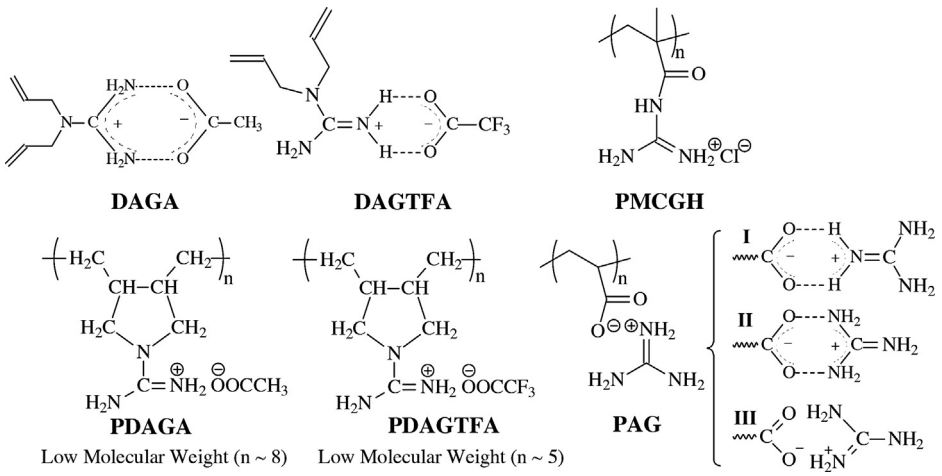

Fig. 1. Guanidine containing monomers and polymers with their resonance structures: diallyl guanidine acetate (DAGA), diallyl guanidine trifluoroacetate (DAGTFA), polydiallyl guanidine acetate (PDAGA), polydiallyl guanidine trifluoroacetate (PDAGTFA), polymethacryloyl guanidine hydrochloride (PMCGH), polyacrylate guanidine (PAG).

Table 1
Amounts of polymers and precursors used in sol–gel synthesis of polymer coated silica particles.

Sample	TEOS (mL)	H_2O (mL)	$C_{polymer}$ (mg/mL)	Stirring time (h)	Gelation time (days)
SiNP	8.57	2.8	–	5	1–2
SiNP@PDAGA-1	8.57	10	44	5	1–2
SiNP@PDAGA-2	8.57	10	57	5	1–2
SiNP@PDAGA-3	8.57	10	77	5	1–2
SiNP@PDAGTFA-1	8.57	10	42	5	1–2
SiNP@PDAGTFA-2	8.57	10	55	5	1–2
SiNP@PDAGTFA-3	8.57	10	76	5	1–2
SiNP@PAG-1	8.57	10	45	5	1–2
SiNP@PAG-2	8.57	10	56	5	1–2
SiNP@PAG-3	8.57	10	77	5	1–2
SiNP@PMCGH-1	8.57	10	46	5	1–2
SiNP@PMCGH-2	8.57	10	57	5	1–2
SiNP@PMCGH-3	8.57	10	78	5	1–2

to too low concentration of sulfasalazine we used other parameters for its loading: 5 mg of dispersed polymer coated SiNPs was incubated with 5 mL of sulfasalazine solution during 20 h at room temperature. The resulting suspension was centrifuged for 10 min at 132,000 rpm. The drug concentration in supernatant solution was monitored by measuring of absorption spectra at the 360 nm. To investigate a pH effect on sulfasalazine loading, pH value was adjusted if needed by NaOH or HCl solution, like for doxorubicin. For increasing of adsorption value of sulfasalazine we used dimethyl sulfoxide (DMSO) solution. For this reason, 20 mg of dispersed polymer coated SiNPs was incubated with 2 mL of sulfasalazine (2 mg/mL) solution for 24 h. The obtained suspension was centrifuged for 10 min at 132,000 rpm and the absorbance of supernatant solution at 360 nm was measured to calculate the amount of adsorbed sulfasalazine.

The entrapment efficiency of doxorubicin and sulfasalazine in silica samples was calculated as follows:

$$\text{Entrapment efficiency}\,(\%) = \frac{\text{initial amount of drug} - \text{residual}}{\text{initial amount of drug}} \times 100\% \quad (1)$$

2.5. Drug release

To study the release of drug molecules, 10 mg of drug adsorbed sample was dispersed within 6 mL of acetate buffer (ABS) in case of pH 3 and 5.1 or in PBS in case of pH 7.4 under gentle stirring at temperature 37 °C. Regularly, the 1 mL of suspension was tested by UV–Vis spectrometer at 485 nm (doxorubicin) or 360 nm (sulfasalazine) and the required volume of fresh buffer (ABS or PBS) was added to keep the conditions.

2.6. Characterization

The images of our samples were obtained using LEO 1550 Scanning Electron Microscope (SEM) which is available in Centre of MicroNano Technology (CMi) of Ecole polytechnique fédérale de Lausanne (EPFL). Before examining, all samples were mixed with ethanol to prepare suspension. The drop of the suspension was adhesive onto copper surface and dried. SEM imaging was performed under a working distance between 3 and 4 mm with acceleration voltages of 3–5 kV. The chamber vacuum was 10^{-7} mbar. We used two signals for SEM imaging: InLens (high resolution detector) and SE2 (topography visualization). Transmission electron microscope (TEM, JEOL 2200FS) was also used for more detailed observation of silica samples. Fourier transform infrared (FT-IR) spectra of the samples were recorded on a Nicolet TM 4700 FTIR spectrometer ("Nicolet", USA) using KBr technique. The nitrogen, hydrogen and carbon contents were determined by an Elemental Analyzer (Thermo Flash 1112 CHNS Analyzer). Thermal gravimetric (TG) analysis and differential scanning calorimetry (DSC) measurements were conducted via STA 449 F3 Jupiter (Netzsch, Germany) in argon atmosphere from room temperature up to 900 °C with a ramp rate of 10 °C/min. An alumina crucible with a cover was used during thermal analysis.

The common formula for determination of grafting yield is as follow:

$$\text{Grafting yield}\,(\%) = \frac{W_1 - W_0}{W_0} \times 100 \quad (2)$$

where W_1 and W_0 represent the weight of initial and grafted substrate, respectively.

In route I, the grafting yield can be estimated by elemental analysis from the content of nitrogen in polymer coated silica particles. $\omega_N = m_N/W_1 \times 100$ (%); m_N is a mass of nitrogen in polymer coated silica (W_1).

$$m_{\text{polymer}} = \frac{1}{3} \cdot \frac{m_N \cdot M_{\text{polymer}}}{M_N}$$

$$\text{Grafting yield} = \frac{W_1 - W_0}{W_0} = \frac{m_{\text{polymer}}}{W_1 - m_{\text{polymer}}}$$

To sum up, we obtained the following equation:

$$\text{Grafting yield}\,(\%) = \frac{\frac{1}{3} \cdot \omega_N \cdot M_{\text{Polymer}}/M_N}{1 - \frac{1}{3} \cdot \omega_N \cdot M_{\text{Polymer}}/M_N} \times 100 \quad (3)$$

where ω_N is nitrogen content in the sample; M_{polymer} and M_N are molecular weight of repeating fragment in polymeric chain and atomic mass of nitrogen.

In route II, the grafting yield can be also determined by thermogravimetric analysis using the following equation:

$$\text{Grafting yield}\,(\%) = \frac{\Delta W_{150} - \Delta W_{800}}{\Delta W_{800}} \times 100 \quad (4)$$

where ΔW_{150} and ΔW_{800} are the weight losses at 150 and 800 °C, respectively.

The zeta-potential of prepared samples were measured using Brookhaven ZetaPlus zeta potential analyzer. All dispersions used for zeta potential measurement were adjusted to the required pH value with HCl and NaOH solutions. Zeta potential measurements were repeated three times. UV–Vis spectra were taken with Varian Cary Bio UV–Vis Spectrophotometer. The pH values were measured by pH meter (Mettler Toledo, Swiss).

3. Results and discussion

3.1. Characterization of polymer coated silica nanoparticles

According to synthetic procedure, we prepared silica samples with three different amounts of grafted polymers (from 18% to 34% estimated by TG and elemental analysis). It was determined that such synthetic procedure allows obtaining 1.61 g of solid product (yield, ~70%) and maximum concentration of polymer should not be more 78 mg/mL otherwise becomes difficult to clean the result material from weakly adsorbed polymer (confirmed by TG analysis) otherwise becomes difficult to clean the resulting material from weakly adsorbed polymer (confirmed by TG analysis). The presence of weakly adsorbed polymer can lead to incorrect estimation of results. After washing and drying, the prepared samples were characterized by FT-IR, elemental and TG-DSC analysis.

The FT-IR spectra of uncoated and polymer coated silicas are presented in Fig. 2. We have shown only IR-spectra of samples with maximum content of grafted polymer. The IR-spectra of samples with lower content of polymer are available as supporting information (Fig. 1S). Analysis of FTIR spectra revealed the broad band in the range 3600–3300 cm^{-1} corresponding to the O–H stretching vibrations of hydrogen-bonded water molecules and SiO–H stretching vibrations [29]. The corresponding Si–OH bending mode is found around 950 cm^{-1}. The band at 1620 cm^{-1} is an indication of adsorbed water, which is also present on the bare silica because of its difficult removal in such experimental conditions. The "bulk" vibrational modes corresponding to SiO_4 groups are observed at 1087–1095 and 800 cm^{-1} (antisymmetric and symmetric Si–O–Si vibrations, respectively), with the bending vibrations near to 460 cm^{-1} [30].

The FTIR spectra of polymer coated silicas show the described modes of amorphous silica and some new frequencies due to presence of guanidine-containing polymers. Minor similar changes were observed in low frequency range (1000–450 cm^{-1}) for all modified samples: broadening and light shifts. In a high frequency range the new bands between 2949 and 2851 cm^{-1} corresponding to intensive asymmetric and symmetric C–H stretching vibrations were emerged. Their discussion is obstructed because of

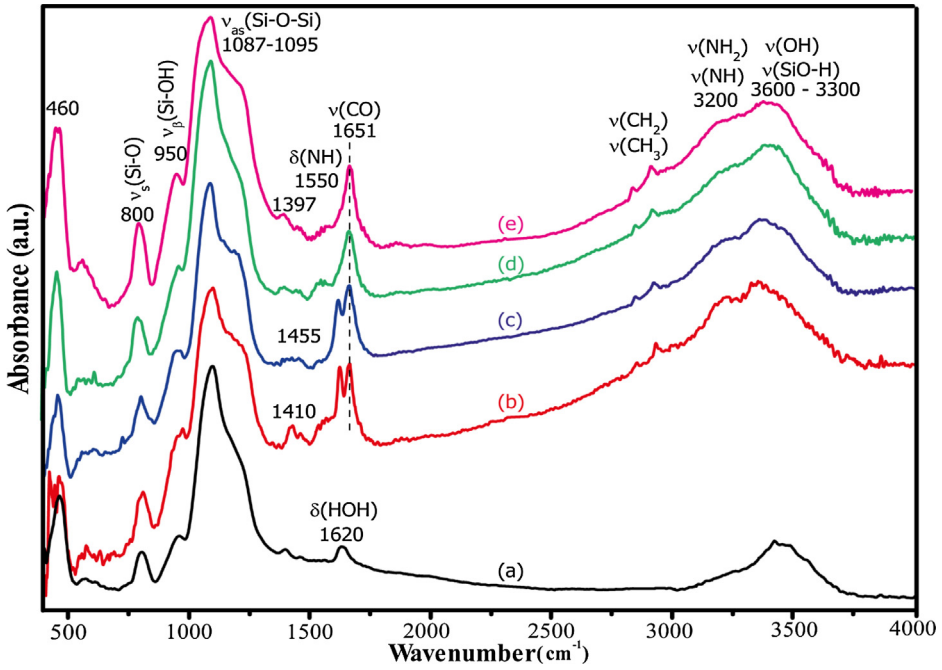

Fig. 2. FT-IR spectra of (a) SiNP, (b) SiNP@DAGA-3, (c) SiNP@DAGTFA-3, (d) SiNP@PAG-3, (e) SiNP@PMCGH-3.

Table 2
TGA and elemental analysis of guanidine-grafted silica particles.

Sample	TGA	Elemental analysis (EA)			Grafting yield (%)	
	Weight loss (%)[a]	H wt.%	C wt.%	N wt.%	TGA[b]*	EA[c]*
SiNP	3.87	0.51	0.12	–	–	–
SiNP@PDAGA-1	14.95	1.74	10.13	3.24	17.8	18.17
SiNP@PDAGA-2	18.64	2.36	11.43	4.21	23.2	24.97
SiNP@PDAGA-3	24.79	3.21	13.97	5.41	33.4	34.49
SiNP@PDAGTFA-1	14.82	1.27	8.29	2.61	17.6	18.69
SiNP@PDAGTFA-2	19.23	1.67	8.89	3.30	24.1	24.88
SiNP@PDAGTFA-3	24.73	2.14	11.71	4.26	33.3	34.52
SiNP@PAG-1	14.96	1.51	5.68	4.97	17.7	18.36
SiNP@PAG-2	18.20	1.83	7.16	6.27	23.1	24.31
SiNP@PAG-3	24.14	2.76	9.45	8.27	33.6	34.76
SiNP@PMCGH-1	14.67	1.42	5.78	4.01	17.8	18.54
SiNP@PMCGH-2	17.95	1.87	7.21	5.01	23.1	24.27
SiNP@PMCGH-3	23.80	2.61	9.49	6.57	33.2	34.36

[a] Weight loss is ranging from 150 to 800 °C.
[b] Determined from the content of nitrogen (N wt %) using Eq. (3); *the values of standard deviation do not exceed 0.1%.
[c] Determined using Eq. (4); * the values of standard deviation do not exceed 0.03%.

strong overlapping by –OH and N–H stretching modes of primary amines (3400 and 3200 cm^{-1}). Latter ones are clearly seen in spectra of modified silica as a shoulder on the left side of the broad band caused by O–H stretching vibrations (between 3120 and 3275 cm^{-1}) and can serve as an evidence of successful inclination of functionalized groups into silica.

Perceptible differences were observed in 1700–1400 cm^{-1} regions. Here all samples demonstrated development of number weak bands at 1397, 1455 and 1550 cm^{-1} while 1620 cm^{-1} band strong increased, up-shifted and in case of SiNP@PDAGA-3 and SiNP@PDAGTFA-3 divided to two bands (Fig. 2). The band around 1410 cm^{-1} can be assigned to the combination mode of ν(C–O) + ν(C–C) vibration. The new peak at 1550 cm^{-1} corresponds to the δ(N–H_2) bending vibrations. The bands in 1700–1600 cm^{-1} range are responsible for carboxylic and amine bonds in all functional groups of grafted polymers. Thus, FT-IR results clearly confirm successful silica surface modification with guanidine containing polymers.

Elemental analysis was performed for polymer coated silica particles to detect the presence of nitrogen, carbon and hydrogen after polymer coating. These results prove the successful grafting of polymer onto silica particles. The quantitative estimation of grafting yield (GY, %) of polymers coated onto silica particles was calculated using the content of nitrogen from elemental analysis (Table 2).

One indication of successful grafting of polymer onto silica can be inferred from thermal analysis. The TGA was also used to determine the percent of organic functional groups chemisorbed on the surface of silica (Table 2).

The TG curves of polymer coated silicas show the mass loss of the organic component as it decomposes upon heating (Fig. 3). The weight loss below 150 °C is due to the removal of physically adsorbed water and surface hydroxyl groups [31–33].

The character of TG curves is identical as for SiNP@PDAGA and SiNP@PDAGTFA and quite different for SiNP@PMCGH and SiNP@PAG. This observation is unambiguously correlated with a structure of grafted polymers. In case of SiNP@PDAGA and SiNP@PDAGTFA the TG shows one strong weight loss which starts at 150 °C and mostly finishes near 400 °C. Around 250 °C the inclination is slightly changed that assumes another process. The long tail after 400 °C was due to the carbonization of the decomposed products to ash. The weight loss below 150 °C due to presence of water on surface is negligible and not influenced by content of polymer. In contrast the SiNP@PMCGH and SiNP@PAG have a quantity of water compared to SiNP, which increases with content of grafted polymer. The TG curves of SiNP@PMCGH and SiNP@PAG are characterized by few steps of weight loss and the temperature of polymer decomposition is much higher than for SiNP@PDAGA and SiNP@PDAGTFA (estimated from the peaks on the DSC curves). It allows to conclude PMCGH and PAG have higher thermal stability than PDAGA and PDAGTFA polymers grafted on silica.

The grafting yield of polymer which was calculated from TG analysis has also been in a good agreement with results of elemental analysis (Table 2). DSC thermograms clearly show the endothermal peak at 80 °C, which is due to weight loss of adsorbed water for SiNP@PDAGA, SiNP@PDAGTFA and SiNP@PMCGH, SiNP@PAG, respectively (Fig. 3). All of them directly related to the occurring mass-loss steps on TG curves. The polymer coated silica particles excepting the SiNP@PDAGA revealed one broad exothermal peak, which is not accompanied by mass loss and appeared between 400 and 600 °C. In this temperature diapason the larger half of grafted polymer is decomposed and it might be that remaining part can rearrange on the surface. This conformation transfer is observed at 424, 482, and near 520 °C for SiNP@PAG, SiNP@PMCGH, and SiNP@PDAGTFA, respectively. Only in case of latter sample this process obviously depends on the content of grafted polymer and shifts to low temperature with its increasing (Fig. 3).

SEM images of uncoated and polymer coated silicas (SiNP@PMCGH-3 and SiNP@PAG-3) with different magnification are presented in Fig. 4a–c and for SiNP@PMCGH-2 and SiNP@PDAGA-3 in supporting information (Fig. 2S). There were no significant differences in SEM images for polymer coated SiNP with change of polymer and its content. On that reason we will discuss using images of two samples. It was observed no particle agglomeration after surface modification. Both uncoated and polymer coated silica particles show spherical shape. The polymer coated silicas (SiNP@PMCGH-3 as an example, Fig. 4b) exhibit a good uniform and monodisperse spherical morphology with an average particle diameter of 300–350 nm. This distribution range is appreciably narrow compared to uncoated silica, which shows size of particles between 250 and 450 nm that indicates positive effect of grafted polymer on monodispersity of formed particles. We suggest that a higher mean diameter and better dispersivity of the polymer coated silica particles might be due to the viscosity and hydrophilic properties of grafted polymers. We also used SE2 signal to observe our polymer coated silicas in the three-dimensional space (SiNP@PAG-3 in Fig. 4c, SiNP@PAG-2 and SiNP@PDAGTFA-3 in Fig. S2). A detailed morphological structure of polymer coated silica was further examined by TEM (Figs. 4d and 2S). The TEM images of SiNP@PAG-3 clearly show excellent spherical shape and amorphous structure.

3.2. Zeta-potential analysis and sulfasalazine and doxorubicin loading

We performed zeta-potential experiments to demonstrate the influence of grafted polymers on charge density of our samples by varying pH values (Fig. 5a). First of all, as it is seen from the results, the polymer coating has a strong effect on surface charge of particles. All polymer grafted silicas excepting the SiNP@PAG have shown the pH increase of zero zeta-potential compared with uncoated SiNP. SiNP@PAG-3 demonstrates negative charge almost in all pH range (from pH 2.6). It means that PAG polymer carries the small negative charges and therefore slightly develops the negative charge net intrinsic to SiNP. In Fig. 5a we placed results only for samples with highest content of grafted polymers but some interesting observation was noted if to analyze the effect from the polymer content on zeta-potential values (Table 1S). At pH 3 absolute value of zeta potential increased with increasing amount of grafted polymers. The weakest effect was found for PAG (ΔZ 3 mV) and strongest for PMCGH polymer (ΔZ 13 mV) which is correlated with

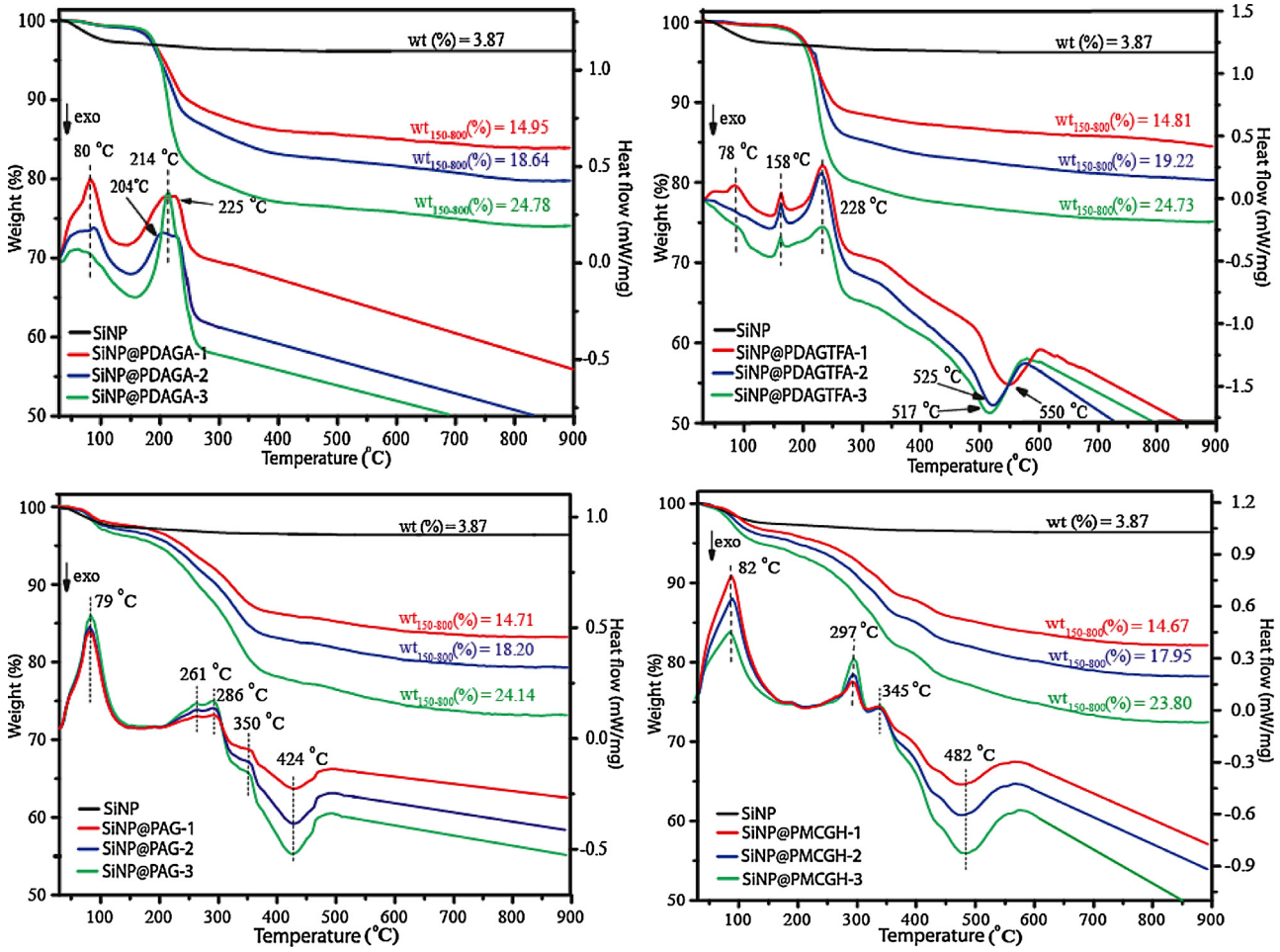

Fig. 3. TG-DSC thermograms for uncoated and polymer coated silica particles. The weight loss for polymer coated silicas was estimated from 150 to 800 °C.

their isoelectric point (ISP), the closer pH of measured solution to ISP – the smaller effect from amount of grafted polymer. The influence of polymer content on zeta-potential decreased for PDAGA, PDAGTFA and PMCGH moving to the pH 5. Finally, it becomes reverse under pH 7.4 excepting SiNP@PAG where grows up (ΔZ 11.9 mV). These correlations support to direct relationship between zeta-potential and amount of grafted polymer. The effect of nature of grafted polymer on zeta potential behavior is also clearly seen in Fig. 5a. As we mentioned, SiNP@PAG-3 has negative potential in wide range of pH though the presence of guanidinium cation. It can be explained by the fact that this cation binds to polyacrylic acid only via electrostatic forces and weak hydrogen bonding, therefore, in aqueous solution PAG easily dissociates onto polyanion of polyacrylic acid and guanidinium cation. The polyanion of polyacrylic acid is strongly grafted on silica particles producing a fixed negative charge [30]. The similar effect of polyacrylic acid was also demonstrated in the case of chitosan-poly(acrylic acid) (CS-PAA) nanoparticles: negatively charged PAA molecules adsorbed onto the surface of CS-PAA nanoparticles resulted in the negative zeta potential [34]. In contrast, other samples, SiNP@PDAGTFA-3, SiNP@PDAGA-3 and SiNP@PMCGH-3, are positively charged particles at pH below 5.2, 5.6 and 6.61, respectively. In this case, guanidinium cation is present directly in polymer networks generating fixed positive charge in polymeric chain. The lower ISPs for SiNP@PDAGTFA-3 and SiNP@PDAGA-3 in comparison with SiNP@PMCGH-3 could be a result not only the nature of polymer but also an increase in molecular weight of used polymer. It has been reported that molecular weight of grafted polymer has impact on surface properties and values of zeta potential [35]. We can conclude that the surface charge of polymer coated silica particles can be adjusted by varying the pH values which suggesting the possibility to control the drug loading and release by changing the pH values. Therefore, we next studied the effect of pH (from 3 to 7.4) on adsorption of sulfasalazine and doxorubicin. The results are shown in Fig. 5b,c.

The drug loading and entrapment efficiency strongly depend on the type of grafted polymer (Fig. 5b,c). Sulfasalazine has a high loading efficiency in the pH range from 3 to 4 while doxorubicin is better adsorbed at pH 6.5–7.4. It is clear that SiNP@PMCGH-3 is capable of loading more amount of sulfasalazine in comparison with other samples and entrapment efficiency of sulfasalazine could reach up to 60% at pH 3. The loading capacity and efficiency for SiNP@PDAGA-3 and SiNP@PDAGTFA-3 is also good whereas SiNP and SiNP@PAG-3 are incapable of loading sulfasalazine, for example, only 0.5 μmol/g of sulfasalazine can be adsorbed by SiNP at pH 3. This fact might be explained by the presence of repulsive electrostatic interactions between drug molecules and silica surface [36]. As it was previously shown the polymer coated silica particles is pH-sensitive and have different charge density by varying value of pH. Sulfasalazine is a negatively charged drug ($pK_a = 2.4$). Therefore, molecules of sulfasalazine can be electrostatically attached only to positively charged nanoparticles. As a result, we observe high loading capacity in case of SiNP@PMCGH-3 under acidic conditions (below pH 5). Otherwise, doxorubicin carries a positive charge ($pK_a = 8.2$) [37] and thereby is capable of electrostatically interacting only with negatively charged particles such as SiNP and SiNP@PAG. However, when pH is higher than 7, all silica nanoparticles exhibited negatively charged density because of the large

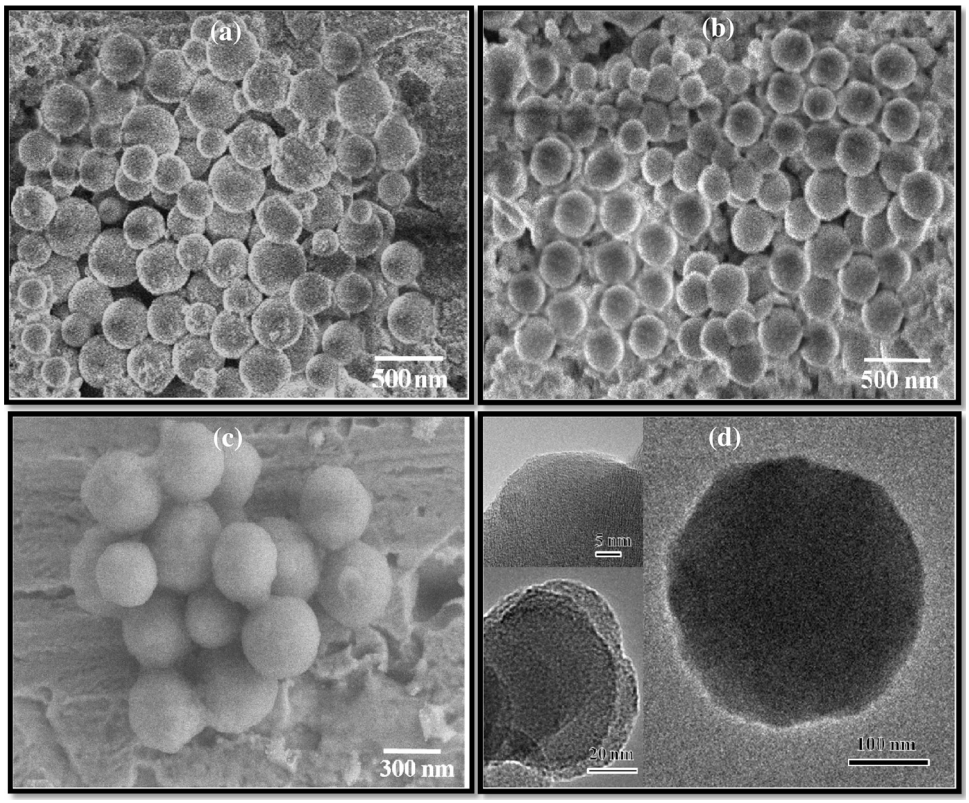

Fig. 4. SEM images of SiNP (a), SiNP@PMCGH-3 (b) and SiNP@PAG-3 (c) with SE2 signal; TEM images of SiNP@PAG-3 (d).

number of de-protonated silanol groups (SiO^-), therefore, strong electrostatic repulsion was generated between sulfasalazine and silica surface which leads to the decrease in sulfasalazine adsorption while molecules of doxorubicin are adsorbed at pH > 7. Thus, such principle of electrostatic binding allows to manipulate the loading efficiency of drugs. The principle of electrostatic binding was also demonstrated in several papers [10,38,39]. For example, the adsorption of lysozyme (+) and bovine serum albumin (−) on silica and AlOOH-coated silica particles–representing negatively and positively charged oxide surfaces – was investigated. It was shown that the adsorption process is affected by electrostatic interactions. An oppositely charged protein adsorbs to the oxide surface in significantly higher amounts whereas proteins of the same charge did not or only in very low amounts adsorbed on an oxide surface [36].

We studied the effect of the amount of grafted polymer on the drug loading. The increase in the amount of grafted polymer leads to simultaneous increase in the drug loading. The drug-loading content of the polymer coated silica nanoparticles are presented as the supporting information in Table 2S. The entrapment efficiency of doxorubicin for uncoated silica is 38% at pH 7.4, whereas in case of SiNP@PAG-3, the entrapment efficiency is greatly increased and reached up to 92% at the same conditions. The maximum adsorption (79.1 ± 2.5 μmol/g) of doxorubicin is observed in case of SiNP@PAG-3 at pH 7.4. Compared with other available materials [3], we suppose that these results are quite promising. For example, Rudzka et al. prepared maghemite nanoparticles encapsulated in a silica shell and gold layer and such material is capable of loading up to 80 μmol/g of doxorubicin [3]. In another work [19], Neetu Sigh synthesized silica nanoparticles modified with polyacrylamid (PAm) and polyethilenglycol (PEG). They showed that the maximum loading of doxorubicin in polymer-coated silica was 52 μmol/g. Also Mahrokh Dadsetan at el reported about preparation of pH-responsive microgels based on a copolymer of oligo(polyethylene glycol) fumarate and sodium methacrylate. Such microgels are capable of loading 67 μmol/g of doxorubicin [40].

The adsorption of sulfasalazine in aqueous solution is lower in comparison with adsorption of doxorubicin (Fig. 5b,c). This is mostly because of sulfasalazine is more hydrophobic molecule and shows less attraction to the hydrophilic surface of silica [41]. To increase the loading of sulfasalazine, we performed experiments in a DMSO solution as it was described in [18,41] for all samples excepting SiNP@PAG. Fig. 5d shows the adsorption of sulfasalazine in a DMSO solution for SiNP, SiNP@PMCGH-3, SiNP@PDAGA-3 and SiNP@PDATFA-3, respectively. As we can see, the loading capacity is higher than for aqueous solution. The maximum adsorption for sulfasalazine molecules is 115.4 ± 3.5 μmol/g in case of SiNP@PMCGH-3. Lee et al. [18] also studied the adsorption of sulfasalazine using trimethylammonium modified silica nanoparticles and his result was 103.1 μmol/g, which is a bit less than we have.

3.3. pH-responsive drug release

The release of doxorubicin was studied at room temperature at pH 5 and 7.4. We used silica samples with loaded doxorubicin at pH 7.4. As it can be seen from Fig. 6a,b the drug release was obviously pH dependent. It is clear that the release of doxorubicin at pH 5 is much faster than that at pH 7.4 which can be associated with the weakening of the electrostatic interaction between silica surface and doxorubicin. The silica samples containing PMCGH, PDAGA and PDAGTFA are characterized by the highest release of doxorubicin at pH 5 which mostly due to the existence of electrostatic repulsion. However, another crucial point influenced the release of doxorubicin should be considered. The solubility of doxorubicin is decreased with decrease of pH. Therefore, besides the influence of electrostatic repulsion, the solubility of doxorubicin has also impact

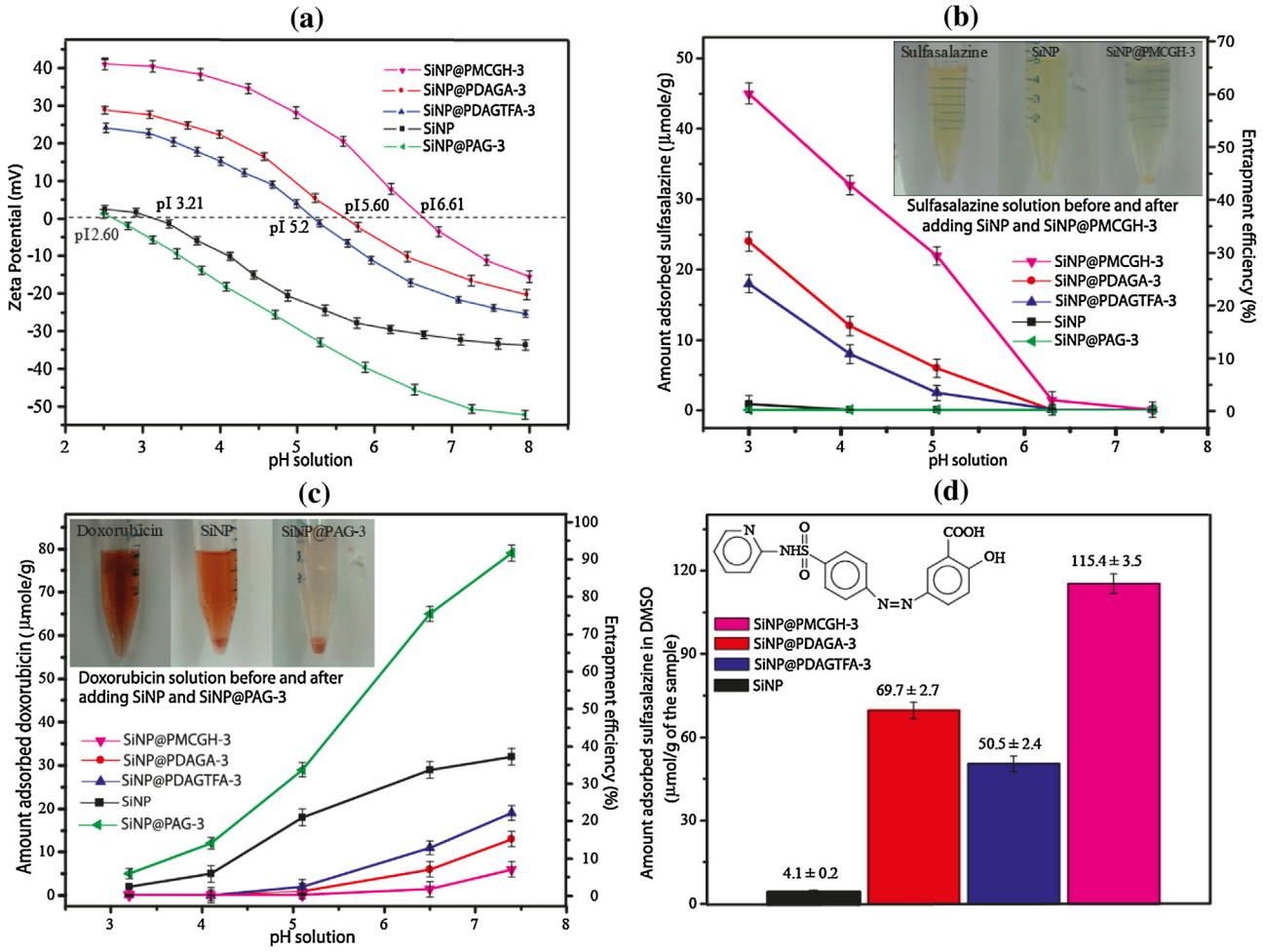

Fig. 5. Zeta potential as a function of pH (a); adsorption of sulfasalazine (b) and doxorubicin (c) at different pH values; sulfasalazine loading in a DMSO solution (d). Values given are mean ± standard deviation ($n = 3$).

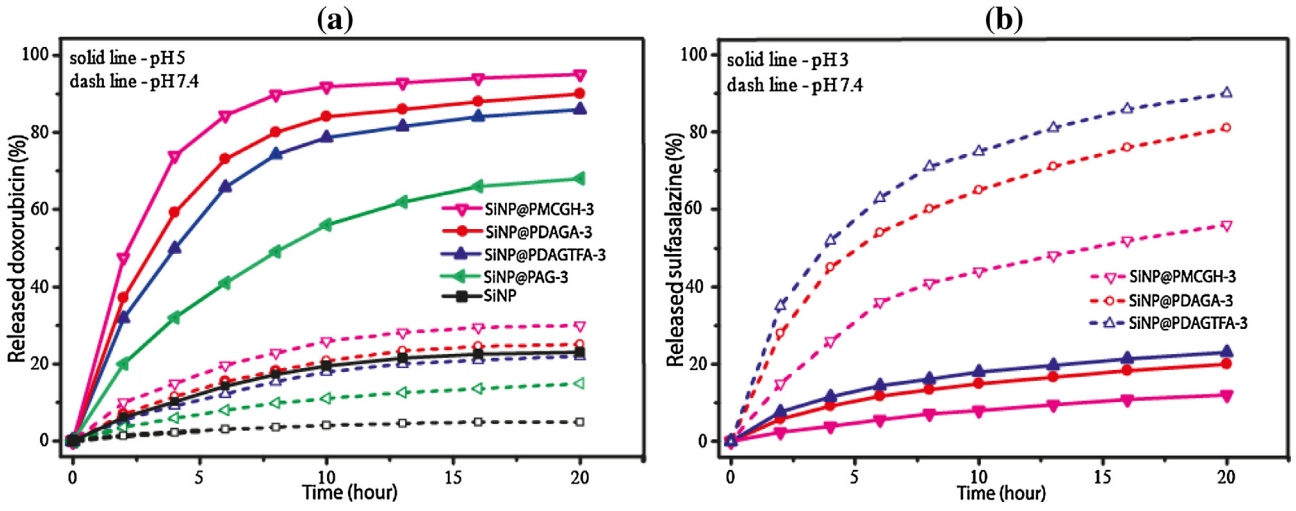

Fig. 6. pH-dependent release of doxorubicin (a) and sulfasalazine (b) for uncoated and polymer coated silica particles.

on fast release under acidic conditions. Nevertheless, 10–14% of loading molecules remained on the surface of polymer coated silicas (SiNP@PMCGH-3, SiNP@PDAGA-3 and SiNP@DATFA-3) for a long period. We suppose that hydrogen bonding retarded the release of doxorubicin. The cumulate release of doxorubicin loaded onto SiNP@PAG-3 at pH 5 and 7.4 was 68% and 13%, respectively. As pH decreased, ionization degree of PAG decreased as well because of the protonation of carboxylic groups in PAG and, therefore, electrostatic interactions between SiNP@PAG and doxorubicin become weaker.

For study of sulfasalazine release we used samples with loaded sulfasalazine in DMSO solution excepting SiNP due to very low drug

loading capacity. Here we demonstrate sulfasalazine release at pH 3 and pH 7.4, respectively. As it can be observed, the extent and the rate of sulfasalazine release were lower when compared with doxorubicin release (Fig. 6b). Sulfasalazine is more hydrophobic drug and, therefore, the hydrophilic environment of the medium will slow up release of sulfasalazine even though electrostatic repulsion takes place. The sulfasalazine release at pH 5 (Supplementary materials, Fig. 3S) did not show significant difference in comparison with sulfasalazine release at pH 7.4, which is affected by high hydrophobic properties of sulfasalazine and weak electrostatic interactions. The extent of sulfasalazine release is basically regulated by the surface charge of polymer coated silicas at different pH value. Therefore, there is a trace release (12–23%) at pH 3 due to high electrostatic interactions between positively charged surface of polymer coated silicas and anionic drug and the release is much higher (55–90%) at pH 7.4 because of electrostatic repulsion between deprotonated silanol groups and negatively charged sulfasalazine, however, again hydrophobic effect plays significant role in reducing release extent of sulfasalazine (especially, in case of SiNP@PMCGH-3) and hydrogen bonding as well.

4. Conclusion

In this work, silica nanoparticles were successfully functionalized with pH-responsive guanidine containing polymers. Polymer coated silica particles do not form agglomerates after modification. The drug loading behavior of doxorubicin (+) and sulfasalazine (−) was investigated at wide range of pH. We demonstrated that drug loading and release depend on the type of grafted polymer and its content in silica nanoparticles. It was confirmed that the principle of electrostatic binding was beneficial for drug loading and drug release as well. The rate and extent of drug release can be controlled by varying the values of pH. Also hydrophobic effect of sulfasalazine prevents high drug release, especially, for SiNP@PMCGH-3. Our data revealed that pH-responsive guanidine containing polymers can be considered as potential candidates for modification of silica particles with following application for cationic and anionic drug encapsulation.

Acknowledgments

We are grateful for support via a stipend of the President of the Russian Federation for study abroad in 2014–2015 (http://www.president-mobility.ru/node/14) and the Ministry of Education and Science of the Russian Federation; special thanks to Aleksandra Radenovic (Laboratory of Nanoscale Biology, EPFL, 1015 Lausanne, Switzerland) and Centre Interdisciplinaire de Microscopie Electronique (CIME) at EPFL for access to electron microscopes (SEM and TEM).

Appendix A. Supplementary data

Supplementary material related to this article can be found, in the online version, at http://dx.doi.org/10.1016/j.colsurfa.2015.03.037.

References

[1] J. Shen, Q. He, Y. Gao, J. Shi, Y. Li, Nanoscale 3 (2011) 4314–4322.
[2] Y. Yang, Y. Jia, L. Gao, J.B. Fei, L.R. Dai, J. Zhao, J.B. Li, Chem. Commun. 47 (2011) 12167–12169.
[3] K. Rudzka, J.L. Viota, J.A. Munoz-Gamez, A. Carazo, A. Ruiz-Extremera, Á.V. Delgado, Colloid Surf. B: Biointerfaces 111 (2013) 88–96.
[4] Y. Yang, W. Song, A. Wang, P. Zhu, J. Fei, J. Li, Phys. Chem. Chem. Phys. 12 (2010) 4418–4422.
[5] Y. Yang, J. Li, Adv. Colloid Interface Sci. 207 (2014) 155–163.
[6] Y. Yang, A. Wang, Y. Jia, G. Brezesinski, L. Dai, J. Zhao, L. Junbai, Chem. Asian J. 9 (2014) 2126–2131.
[7] D. Yang, W. Chen, J. Hu, J. Phys. Chem. B 118 (2014) 12311–12317.
[8] Q. Zhang, K.-G. Neoh, L.-Q. Xu, S. Lu, E.-T. Kang, R. Mahendran, E. Chiong, Langmuir 30 (2014) 6151–6161.
[9] T. Zhou, X. Zhou, D. Xing, Biomaterials 35 (2014) 4185–4194.
[10] H. Meng, M. Liong, T. Xia, Z. Li, Z. Ji, J.I. Zink, A.E. Nel, ACS Nano 4 (2010) 4539–4550.
[11] Y. Gao, Y. Chen, X. Ji, X. He, Q. Yin, Z. Zhang, J. Shi, Y. Li, ACS Nano 5 (2011) 9788–9798.
[12] A. Baeza, E. Guisasola, E. Ruiz-Hernández, M. Vallet-Regí, Chem. Mater. 24 (2012) 517–524.
[13] Y. Jiao, J. Guo, S. Shen, B. Chang, Y. Zhang, X. Jiang, W. Yang, J. Mater. Chem. 22 (2012) 17636–17643.
[14] K.-N. Yang, C.-Q. Zhang, W. Wang, C. Paul, J.-P. Zhou, X.-J. Li, Cancer Biol. Med. 11 (2014) 34–43.
[15] C. Graf, Q. Gao, I. Schütz, C.N. Noufele, W. Ruan, et al., Langmuir 28 (2012) 7598–7613.
[16] B. Chang, J. Guo, C. Liu, J. Qian, W. Yang, J. Mater. Chem. 20 (2010) 9941–9947.
[17] L. Tang, J. Cheng, Nano Today 8 (2013) 290–312.
[18] C.-H. Lee, L.-W. Lo, C.-Y. Mou, C.-S. Yang, Adv. Funct. Mater. 18 (2008) 3283–3292.
[19] N. Singh, A. Karambelkar, G. Luo, K. Lin, J.S. Miller, C. Chen, S. Sailor, S.N. Bhatia, J. Am. Chem. Soc. 133 (2011) 19582–19585.
[20] Y. Luo, Q. Wang, Int. J. Biol. Macromol. 64 (2014) 353–367.
[21] B. Singh, G.S. Chauhan, S. Kumar, N. Chauhan, Carbohydr. Polym. 67 (2007) 190–200.
[22] K. Knop, R. Hoogenboom, D. Fischer, U.S. Schubert, Angew. Chem. Int. Ed. 49 (2010) 6288–6308.
[23] C. Müller, K. Leithner, S. Hauptstein, F. Hintzen, W. Salvenmoser, A. Bernkop-Schnürch, J. Nanopart. Res. 15 (2012) 1353.
[24] N.A. Sivov, Biocide Guanidine Containing Polymers: Synthesis, Structure and Properties, CRC Press, 2006, pp. 151.
[25] K.E. Locock, T.D. Michl, J.D. Valentin, K. Vasilev, J.D. Hayball, Y. Qu, A. Traven, H.J. Griesser, L. Meagher, M. Haeussler, Biomacromolecules 14 (2013) 4021–4031.
[26] A.S. Timin, A.V. Solomonov, E.V. Rumyantsev, J. Polym. Res. 21 (2014) 400–409.
[27] A.M. Carmona-Ribeiro, L.D. Melo Carrasco, Int. J. Mol. Sci. 14 (2013) 9906–9946, http://dx.doi.org/10.3390/ijms14059906.
[28] A.S. Timin, et al., Ind. Eng. Chem. Res. 53 (2014) 13699–13710.
[29] R. Mellaerts, et al., Langmuir 24 (16) (2008) 8651–8659.
[30] J. Zhou, et al., Mater. Lett. 62 (2008) 2910–2913.
[31] M.Z. Kassaee, H. Masrouri, F. Movahed, Appl. Catal. A 395 (2011) 28–33.
[32] A.S. Timin, et al., Mater. Chem. Phys 147 (2014) 673–683.
[33] D. Schmaljohann, Adv. Drug Deliv. Rev. 58 (2006) 1655–1670.
[34] Y. Hu, X. Jiang, Y. Ding, H. Ge, Y. Yuan, Ch. Yang, Biomaterials 23 (2002) 3193–3201.
[35] G. Mittal, D.K. Sahana, V. Bhardwaj, M.N. Ravi Kumar, J. Control Release 119 (2007) 77–85.
[36] H. Tanga, J. Guoa, Y. Sunb, B. Changa, R. Qingguang, W. Yanga, Int. J. Pharm. 421 (2011) 388–396.
[37] Q. Jianing, Y. Ping, H. Fen, Y. Chuiliang, H. Chong, Int. J. Pharm. 393 (2010) 176–184.
[38] H. Meng, W.X. Mai, H. Zhang, M. Xue, T. Xia, S. Lin, X. Wang, Y. Zhao, Z. Ji, J.I. Zink, A.E. Nel, ACS Nano 7 (2013) 994–1005.
[39] K. Rezwan, L.P. Meier, L.J. Gauckler, Biomaterials 26 (2006) 4351–4357.
[40] M. Dadsetan, K.E. Taylor, C. Yong, Z. Bajzer, L. Lu, M.J. Yaszemski, Acta Biomater. 9 (2013) 5438–5446.
[41] C. Shih-Hsun, L. Wei-Neng, Ch. Li-Ming, L. Chia-Hung, J. Mater. Chem. 21 (2011) 7130.